JMEPEG (1992) 1:113-121

Heat-Resistant Dispersion-Strengthened Copper Alloys

Joanna Groza

Processing methods for producing dispersion-strengthened (DS) copper alloys with high strength, high conductivity, and good long-term stability at elevated temperature are reviewed. Particle size and stability are related to material characteristics and processing route. Physical and mechanical properties of DS copper alloys are directly associated with microstructural features such as particle volume fraction, stability, size, solubility in the matrix, and interfacial properties. New avenues for DS copper alloys design are suggested based on thermal conductivity concept and recent Rosler-Artz theory of high-temperature strength.[1]

1 Introduction

HEAT-RESISTANT and stable materials with high thermal conductivity are in continuous demand for actively cooled parts used in a variety of existing and potential applications. They include, for example, rotating source neutron targets, plasma interactive components in fusion power systems, and combustion chamber liners, nozzle liners, and leading edges in advanced aircraft and rocket propulsion systems. For these applications, copper stands out as a prime candidate, because it has the highest thermal conductivity among the structural materials. Copper alloys also bring the advantage of low elastic modulus, which minimizes thermal stresses, and good resistance to neutron displacement damage.

Various mechanisms to achieve long-term, high-temperature strength in copper alloys have been considered. Conventional strengthening methods such as cold working and precipitation hardening are not useful for high temperatures due to the effects of recrystallization and particle coarsening and dissolution, respectively. Solid solution hardening significantly lowers the thermal conductivity of copper. Therefore, the primary attention has been centered on fiber or dispersion strengthening (DS). The latter is the major focus of this review.

Dispersion strengthening is usually described as a method of strengthening based on the even distribution of extremely fine particles in a matrix at 0.01 to 0.15 volume fraction. For room-temperature purposes, this class of materials may easily incorporate precipitation-hardened alloys, in which precipitates are efficient dislocation obstacles. In contrast, at high temperatures, the definition must consider dispersoid stability within the matrix in service conditions. Maintaining the uniform distribution and size of the dispersoids is more important than particle volume fraction for high-temperature strength. As a result, the volume fraction is often less than 5%, which evidently is beneficial for maintaining a high conductivity of the entire material.

To date, a variety of DS copper-base alloys have been produced and studied.[2-16] However, only the commercially available Cu-Al_2O_3 alloys produced by internal oxidation have been reviewed in detail.[3,17] Renewed interest in dispersion-strengthened copper alloys has resulted in numerous recently published articles or papers presented at scientific conferences.[4-16] In the alloys described in these papers, strengthening is usually achieved by the introduction of one type of particle such as a ceramic, intermetallic compound, or a refractory metal phase.

This review begins with a brief description of processing methods (other than classical internal oxidation, which is covered by other reviews) to obtain DS copper alloys. The primary focus of this paper is devoted to particle characterization and behavior, with the aim of determining physical and mechanical properties of DS copper alloys. Finally, means to achieve the desired combination of high-temperature strength and high conductivity in copper alloys are suggested.

2 Processing Methods

Copper alloys reinforced by ceramic particles (oxides or carbides) and intermetallic compounds have been produced by internal oxidation, chemical precipitation, mechanical alloying, rapid solidification, and proprietary melting processes.

Chemical precipitation was used to obtain thoria dispersed copper by precipitating copper on individual ThO_2 particles.[2] No Cu-ThO_2 reaction is involved during chemical precipitation or subsequent hot or cold processing, so that the final particle size is strictly dependent on initial thoria particle size. The initial ThO_2 particle size reported by Fuschillo and Gimpl was 50 nm.[2] As will be shown later, chemical precipitation produces good high-temperature mechanical properties, but is expensive.

Mechanical alloying (MA) is a solid-state, high-energy ball milling process that consists of repeated deformation, welding, and fracturing of original components. As a result, a very fine mixing of the components, and hence a controlled dispersion of second phase, is obtained. Moreover, MA also permits the selection of alloy composition without regard to liquid or solid solubility limits, thereby significantly expanding the options for dispersoid selection. Consequently, the use of MA has been very successful in commercially producing dispersion-strengthened nickel, iron, and aluminum alloys.[18] However, only preliminary work has been performed in mechanically alloyed dispersion-strengthened copper. For instance, Schroth and Franetovich obtained a homogenous distribution of 20 to 50 nm ZrO_2 particles with interparticle spacings on the order of 100 nm in Cu-4 vol% ZrO_2 and about 30 nm particles of Al_2O_3 in Cu-2 vol% Al_2O_3.[4] Morris and Morris have produced mechanically alloyed copper with 10 to 15 nm diboride particles (CrB_2, ZrB_2, and TiB_2) that have interparticle spacings in the range of 72 to 94 nm.[5]

Joanna Groza is with the Department of Mechanical, Aeronautical and Materials Science & Engineering, University of California, Davis, California.

Often MA has been combined with other techniques to create dispersion-strengthened copper alloys. For example, Schaffer and McCormick obtained CaO-dispersed copper by combustion synthesis during mechanical alloying of CuO and Ca.[6,19] Mechanical alloying leads to an intimate mixing of reactant powders that enables the reduction reaction to occur at interfaces of layered reactant particles: CuO + Ca = Cu + CaO. The high reaction enthalpy (ΔH = –473 kJ/mol) allows a sustained combustion reaction to take place. The relatively coarse CaO particles obtained immediately after combustion (100 μm) are broken down during subsequent mechanical alloying. Although a recent paper considers the mechanism and kinetics of the combustion reaction,[19] detailed study of reaction kinetics and its dependence on mechanical alloying parameters is still required. We expect this method to be more widely used based on its potential to enhance the combustion reaction by intimate mixing of components and to refine the final product.

Mechanical alloying also has been used as a first step before internal oxidation to ensure a "homogeneous" mixing of reactive elements prior to final reaction (reaction milling).[7,20] The diffusion paths are thus reduced during subsequent heat treating when oxides are formed. In contrast to MA oxide dispersion-strengthened copper, the oxide particle size is dependent on alloy chemistry and heat treating conditions for oxidation and varies in the same way as for regular second-phase precipitates, *i.e.*, dispersed particles coarsen at high temperatures. The oxide structure depends on heat treating conditions as well. For instance, in Cu-Al-O alloys, both α- and γ-Al_2O_3 particles are obtained depending on heat treatment conditions,[7,21] and complex oxides such as $Fe(Al, Cr)_2O_4$ are also found.[7] The average oxide particle size in these alloys is 10 to 30 nm as compared to about 10 nm in commercially available internally oxidized alloys (*e.g.*, GLIDCOP* alloys).[9,20] An earlier observed tendency of fine oxide particle to agglomerate during the internal oxidation step was noted by Takahashi and co-workers[7] thus confirming earlier observations of Komatsu and Grant. However, finer oxide particles may be obtained if proper alloying additions are made. For instance, Takahashi and co-workers added transition elements such as Ti to refine Al_2O_3 particles in Cu-Al-Ti alloys.[19] Although this refining mechanism has not been studied extensively, Daneliya *et al.* proposed that precipitation of TiO_2 at the Al_2O_3-matrix interface is responsible for oxide refinement by adsorption of titanium atoms on the surface of growing Al_2O_3 nuclei.[21]

Carbide particles may be obtained by internal carburization, a process similar to internal oxidation. In Japan, Takahashi and co-workers have obtained carbides in copper by chemical reaction of milled carbon additions to copper and carbide making metal powders such as Nb, Ta, Ti, and Zr.[8] Carbide particle formation is kinetically similar to oxide formation in internal oxidation. However, carbide growth rate as a function of temperature is significantly lower than that of oxides, and no carbide agglomeration was observed. Differences in carbide growth rates have been noticed; for example, ZrC particles have a higher tendency to grow than TiC.[8] Nevertheless, final carbide particle size is very small, on the order of 3 to 20 nm.

* GLIDCOP is a registered tradename of SCM Metal Products, Cleveland, Ohio.

Intermetallic-reinforced copper has been obtained by both MA and rapid solidification (RS) techniques. As already described, mechanical alloying has been used by Morris and Morris to uniformly incorporate 10 to 15 nm diboride particles (CrB_2, ZrB_2, and TiB_2) in a copper matrix.[5] Ellis and Michal[15,16] produced a series of copper alloys with Cr_2Nb as dispersoids by the chill block melt spinning technique. Cr_2Nb was selected based on its stability, total solubility in liquid copper, and minimum solubility in solid copper. Because both Cr and Zr are soluble in a copper matrix, the Cr/Zr ratio is critical to obtaining only Cr_2Nb precipitates in a pure copper matrix. Although the bulk Cr_2Nb particles precipitate from the liquid, second phase precipitation and coarsening still occur during subsequent heat treatments and follow the aging kinetics. Consequently, precipitates are bimodally distributed with a typical size of 10 to 50 nm. In this sense, it is only marginally appropriate to include the RS alloys in the class of dispersion-strengthened alloys that are of interest to this review. Nevertheless, they will be used for comparison with other dispersion-strengthened copper alloys.

Proprietary techniques in which a fine distribution of intermetallics is obtained in liquid copper have been used to produce the MXT alloys series (Cu-TiB_2)[9] and XD alloys.[22,23] In the latter case, reinforcing particulates are formed *in situ* in the liquid phase. The environment is carefully controlled so as to ensure a contaminant-free interface between particles and the matrix. The particle-reinforced matrix liquid is then atomized and consolidated by the usual powder techniques. Although no data on particle size are available, studies on the other XD alloys indicate a strong dependence of dispersoid size on the temperature of subsequent extrusion.[22]

A proprietary method of producing Cu-Al_2O_3 alloys was recently developed by Blossom.[10] The base material was raw copper oxide, which was reduced to a fine, high-purity copper powder that was further dispersion strengthened by alumina. No data on particle size are available.

To date, many investigations have focused on copper reinforced by refractory metal particles. Usually, these alloys contain refractory metal in excess of its solubility limit in copper and are obtained by melting techniques or mechanical alloying. Melting techniques include rapid solidification and proprietary methods.[12,24-26] Cu-15 vol% Nb or Ta has been obtained by proprietary melting methods with particle sizes of 1 to 2 μm.[26] Morris and Morris compared the supersaturation, particle distribution, and stability of rapidly solidified and mechanically alloyed Cu-Cr alloys.[12] They achieved 5 at.% Cr in copper by melt spinning, with about 3 at.% Cr formed in primary solidification, and the remaining in supersaturated solid solution. Using this method, a bimodal distribution of particles is found with primary solidification particles of about 50 nm and secondary particles of about 18 nm distributed mainly on the grain boundaries. Similarly, a trimodal distribution of chromium particles has been reported by Patel and Diamond in rapidly solidified Cu-5 at.% Cr.[13] The largest primary particles (25nm) are distributed at grain boundaries, the intermediate (10 to 15 nm), secondary ones are distributed at subgrain boundaries, and fine 5 to 6 nm secondary particles are uniformly distributed within the subgrains. Precipitate-free zones are observed on both subgrain and grain boundaries. Although in both cases secondary precipita-

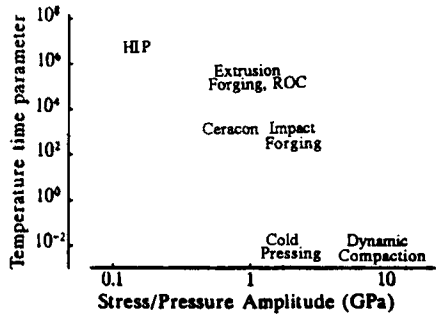

(a)

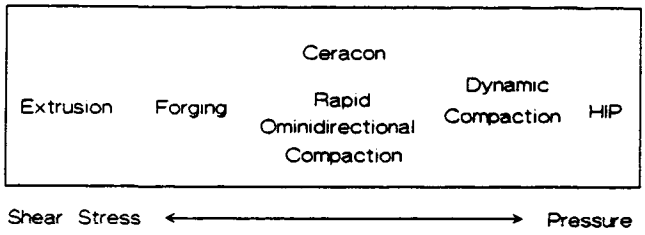

(b)

Fig. 1 Schematic comparisons of consolidation techniques on the basis of (**a**) stress, pressure, and temperature and (**b**) whether shear or pressure forces are applied. Adapted from Ref 27.

tion occurs during solidification, we assume that the trimodal distribution is due to a slightly lower solidification rate than that of alloys with bimodal distribution. Annealing changes the above as-cast distribution pattern because of the fastest coarsening rate exhibited by the smallest secondary particles. Again, because solid-state precipitation occurs in these RS alloys, they can be only marginally included in the DS alloys class.

Copper alloys produced by mechanical alloying typically contain 5 to 15 at.% bcc refractory element.[12-14] In a detailed study on mixing of bcc refractory element and copper matrix, Morris and Morris concluded that strong chemical interaction across the particle-matrix interface will transfer the applied forces to the second-phase particle, thereby deforming it more effectively. This interaction may be measured by the heat of formation of an imaginary copper-bcc element compound. A large negative heat of formation leads to a refined degree of mixing as in the case of Nb or Ta in Cu, followed by V and Cr. For instance, V particle size is around 5 to 10 nm after 12 hr of milling. In contrast, Mo and W are poorly refined, with particle size ranging from 20 to 500 nm after the same milling time.[14] However, Diamond and Patel report a fine mixing of 40 wt% W in copper by MA, namely an interlamellar spacing of about 0.5 μm after milling for 50 hr.[13] The estimated particle size is about 85 nm. Refinement of Mo to submicron size in Cu-10% Mo alloy has been reported by Schroth and Franetovic after milling for 18 hr.[4]

In spite of some solubility of the bcc elements in the copper matrix, these MA materials may still be considered dispersion-strengthened alloys. This statement will be better demonstrated later by considering the high stability of refractory metal particulates both during consolidation and under service conditions.

3 Consolidation Processes

Dispersion-strengthened copper alloys are usually produced in powder form. Copper powders are easily consolidated by common methods such as hot pressing, rolling, extrusion, swaging, and hot isostatic pressing (HIP), as well as by unconventional methods that include shock consolidation or the proprietary Ceracon process. To compare the possible consolidation processes, the diagram of stress, pressure, and temperatures used to achieve compaction is presented in Fig. 1(a). A second comparison of the consolidation techniques made on the basis of forces imposed, specifically on the pressure and shear components of forces, is shown in Fig. 1(b). The ideal consolidation technique requires a sufficient hydrostatic pressure to achieve densification in the desired temperature-time combination, whereas a large shear component will cause fracturing of surface oxides leading to effective bonding. The breaking of surface oxides is less important to copper than to aluminum, for instance, because copper surface oxides are easily reduced. As examples, copper powders are consolidated by vacuum hot pressing,[13-16] hot rolling,[16] hot extrusion,[5,12,14] hot swaging,[4] or HIP[13] at moderate temperatures (823 to 1273 K) and pressures (69 to 240 MPa).

4 Particle Stability

For high-temperature applications, retention of the fine particle size during processing and under service conditions is a major requirement. In this sense, the coarsening rate of a dispersoid controls the useful life of the material. At the same time, diffusion of elements from dispersoids into the matrix significantly degrades thermal conductivity of the copper alloy. Similarly, undesirable chemical reactions at the particle interface modify the interface, thereby compromising high-temperature mechanical properties. Therefore, for high-temperature use, the dispersoid phases must be stable and resist coarsening.

The coarsening of a constant volume fraction of particles is described by the Lifshitz-Slyozov-Wagner (LSW) equation for the case when solute diffusion through the bulk material is the controlling process:[28,29]

$$(\Delta r)^3 = \frac{8K\gamma CVDt}{9RT} \quad [1]$$

where Δr is the change in particle radius during annealing at the temperature T for the time t, K is a constant, γ is the particle-matrix interface energy, C is the solubility limit, V is the molar volume of particle, D is the diffusivity, and R is the gas constant.

Morris and Morris applied the LSW formula to calculate particle coarsening in Cu-Cr and Cu-Nb (Fig. 2a and b).[5,12] Reasonably good agreement between calculated and measured particle sizes with respect to temperature has been obtained for both systems. The higher resistance of niobium particles to coarsen-

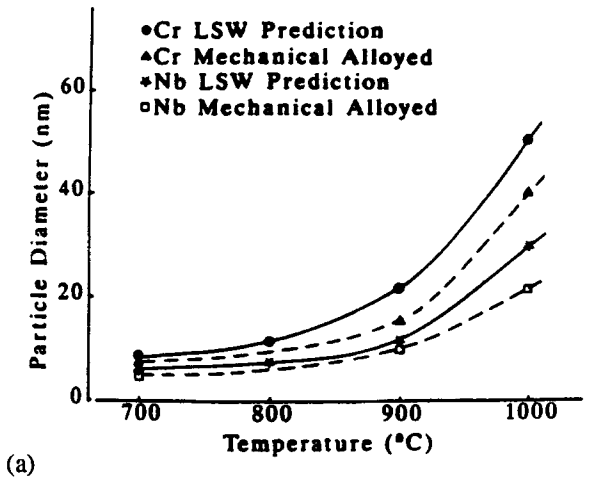

(a)

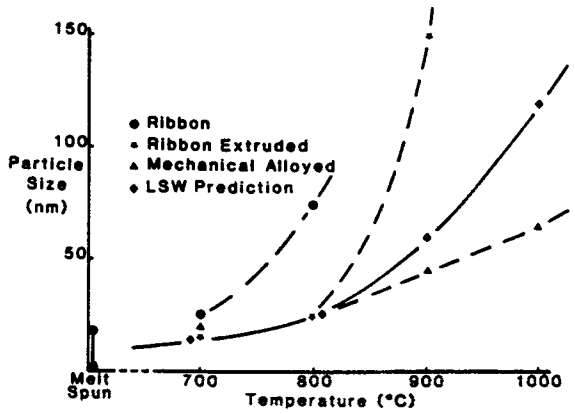

(b)

Fig. 2 (a) Comparison of theoretical and experimental particle coarsening for Cu-Cr and Cu-Nb systems (from Ref 5). (b) Comparison of theoretical and experimental particle coarsening in RS ribbon, extruded RS, and MA Cu-Cr alloys. From Ref 12.

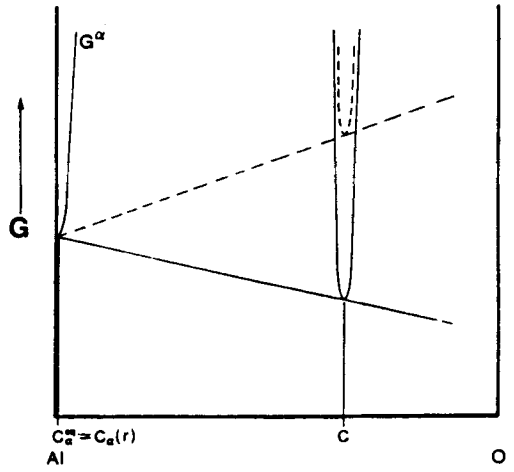

Fig. 3 Free energy vs composition diagram for insoluble particle and effect of the increase in particle solubility. From Ref 30.

ing is explained in terms of the lower solubility and lower diffusivity of niobium in copper relative to chromium. These two factors—solubility and diffusivity—are the key factors in the LSW formula as it considers the growth of larger spherical particles by dissolution of small particles.

To illustrate the role of solubility, it is interesting to note that it would require hundreds of years for Al_2O_3 dispersoids to dissolve in a nickel matrix at 1000 K, as opposed to Ni_3Al dissolution in 100 sec.[30] This result may be understood if we consider the free energy vs composition diagram for insoluble second phases (Fig. 3). It may be seen that the increase in solubility in the matrix associated with small particles as compared to large particles due to the Gibbs-Thompson effect is negligible. In other words, the diffusion gradient for insoluble large particles coarsening at the expense of smaller ones is extremely small. As such, Morris and Morris have found experimentally that particle coarsening rate is very low in MA copper containing insoluble diboride dispersoids as compared to MA binary alloys such as Cu-Nb.[5]

When such experimental data on particle coarsening are not available, some indirect indications may be considered to show that no significant particle coarsening or dissolution occurs in copper alloys that are dispersion strengthened by insoluble particles. For instance, the variation of resistivity or thermal conductivity with temperature is the same in pure copper and Cu-ThO_2 up to 1073 K or Cu-Al_2O_3 up to 573 K (Fig. 4).[2,3] However, at higher temperatures (1313 K), the coarsening rate of Al_2O_3 in GLIDCOP alloy A15 was reported by Stephens *et al.* to be related to changes in oxide chemistry after long-time annealing.[31] Indeed, γ-Al_2O_3 transformed to a new $9Al_2O_3 \cdot 2B_2O_3$ compound. Similarly, the above authors have observed a transformation of TiB_2 toward stoichiometric proportions in MXT-5 alloys by long-time annealing at 1313 K. It is worthwhile to note that the alumina dispersoid particles remain small (about 50 nm), even when recrystallization of the matrix takes place.[32] The same observation was made for secondary recrystallized MA Al-Al_4C_3 alloys by Slesar and co-workers.[33]

Because the coarsening rate is directly proportional to the diffusivity of the solute in the matrix, the benefits of using low-diffusivity elements or compounds with at least one element that diffuses slowly in the matrix are obvious. However, for the same dispersoid type, hence the same diffusivity, the processing route may affect the coarsening rate. For instance, Morris and Morris compared the stability of Cr particles obtained by MA and RS processing during subsequent consolidation of Cu-5 at.% Cr alloy (Fig. 2b).[12] They attribute the faster coarsening rate of RS vs MA alloys at high temperatures to particle distribution in RS materials, *i.e.*, mainly at grain boundaries and at triple points. As already mentioned, this distribution is favored by liquid and solid-state precipitation processes due to nucleation requirements. On the other hand, MA leads to a more uniform distribution of particles, thus minimizing the number of coarse particles

that are favored to grow. The slow rate of coarsening in MA Cu-Cr alloys is even more obvious when compared with conventional Cu-Cr alloys that are known for their overaging effects due to the high diffusivity of Cr in Cu. Patel and Diamond found the fine structure of tungsten particles in Cu-40% W alloy has also been preserved after powder consolidation, although no data were reported.[13]

As already seen, the coarsening rate of a second phase varies with the processing method by which the second-phase particles are dispersed within the copper matrix. Therefore, we assume that the same particles in different alloys have dissimilar interfacial energies, or the interfacial energy is dependent on processing route. For instance, mechanically introduced dispersoids are expected to have a high interfacial energy value, because they are always incoherent. It is also noteworthy that the extremely fine grain size is preserved during extrusion of MA alloys probably due to dispersoid particle pinning.[4,12] For instance, the grain size in MA Cu-5 at.% Cr was 0.3 μm, whereas the RS alloy had a grain size of 4 μm after extrusion at the same temperature.[12] The consolidated MA Cu-ZrO_2 alloy revealed an extremely fine-grained microstructure, with grain sizes varying from 0.2 to 0.5 μm.[4]

The particle growth rate can be used as a criterion to assess the difference between DS and precipitation-hardened alloys. As already stated, the former involves a notably less soluble second phase than the latter. Furthermore, for the same second phase such as Cr in Cu-Cr alloys,[12] the lower coarsening rate in MA materials justifies including them in the DS alloy class. At this point, earlier classification of RS Cu-Cr_2 Nb alloys as precipitation strengthened may be better understood. In these alloys, the initial bimodal size distribution in the range of 16 to 50 nm undergoes a significant coarsening to 100 to 400 nm during consolidation near to the eutectic point.[15] On this basis, we exclude these materials from the DS alloy class.

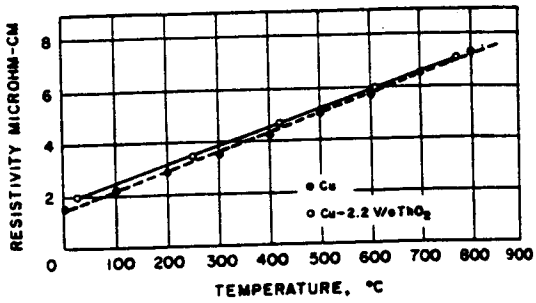

(a)

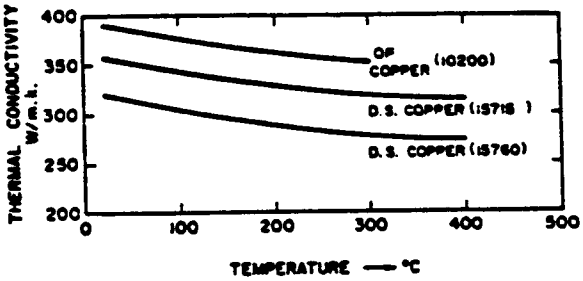

(b)

Fig. 4 Resistivity (**a**) and thermal conductivity (**b**) vs temperature for Cu-2.2% ThO_2 (**a**) and GLIDCOP alloys (**b**). From Ref 2 and 3.

5 Physical and Mechanical Properties

Good thermal conductivity and high-temperature strength are the two primary properties sought in DS alloys. The former is essential to maximize the efficiency of active cooling and minimize thermal strains in the material. As expected, a pure copper matrix is the first requirement for high thermal conductivity. As particles are incoherent, stable, and do not react with the copper matrix, dispersion-strengthened alloys may be considered particulate composites for property calculations. Therefore, the thermal conductivity of a composite with spherical second-phase particles may be calculated using the following formula given by Schroeder:[34]

$$\sigma = \sigma_m \frac{1 + 2f\dfrac{1 - \sigma_m/\sigma_p}{2\sigma_m/\sigma_p + 1}}{1 - f\dfrac{1 - \sigma_m/\sigma_p}{2\sigma_m/\sigma_p + 1}} \qquad [2]$$

where σ_m and σ_p are matrix and particle conductivities, respectively, and f is the dispersoid volume fraction. This formula was initially derived for electrical conductivity. Although the thermal conductivity in metals is determined by both electron flow and lattice heat transfer, only electrons are responsible for heat flow at high temperatures. Therefore, the linear Weidemann-Franz law, which relates thermal to electrical conductivity, may be used safely. The above formula was verified to give accurate results for $f < 5\%$ in Al-Al_2O_3 alloys for which experimental measurements of electrical resistivity were available.[35] However, in most of DS copper alloys, the experimental thermal conductivity is substantially less than the calculated value obtained using Eq 2, as shown in Table 1.

There are three reasons that the measured conductivities are lower than the calculated values: cold worked matrix, impure matrix, and electron scattering from particle-matrix interfaces. For GLIDCOP alloys and Cu-ThO_2 alloys, the first assumption is excluded, because the linear dependence of conductivity with temperature demonstrates no recovery phenomena up to 673 and 1073 K, respectively (Fig. 4).[2,3] Our previous measurements showed that resistivity is a very sensitive function of cold work in copper alloys, and recovery occurs before 673 K.[36] The second assumption was considered for Cu-ThO_2 alloys by Fuschillo and Gimpl[2] and is probably attributed to copper impurification during the precipitation process. In Cu-TiB_2 alloys (MXT-5), the matrix contains residual boron, which perhaps is

Table 1 Calculated and Experimental Thermal Conductivities of Dispersion-Strengthened Copper Alloys

Alloy	f, %	σ/σ_{Cu}, % Calc	Exp	Ref
Cu-Al_2O_3	0.7	99	93	3
	2.7	96	78	3
Cu-TiB_2	5	94	~82	9
Cu-ThO_2	2.2	97	85	2

responsible for lower than calculated conductivity. We assume that some residual elements in the copper matrix after internal oxidation may also explain lower than calculated conductivities in Cu-Al_2O_3 alloys. Nevertheless, this assumption needs verification. The third assumption seems more credible at least for the Cu-ThO_2 alloy, which reaches pure copper conductivity at 1073 K (Fig. 4a).[2] Fuschillo and Gimpl calculated that the effect of interface scattering on particle sizes of 50 nm is negligible at room temperature at low volume fractions ($f < 5\%$). However, because at high temperature the electron mean free path decreases, the last assumption may be the only one accounting for the conductivity variation in Fig. 4(a). A similar conclusion was drawn by Karasek and Bevk for filamentary Cu-Nb composites.[37] Even if the third assumption is realistic, its role at high temperature is insignificant. Indeed, as shown in Fig. 4(a), the difference in conductivities of dispersion-strengthened copper as compared to pure copper vanishes at high temperature. The above discussion strengthens the point that pure copper matrix and stable dispersoids are needed for high thermal conductivity. From Fig. 5, there is no doubt that Cr_2Nb behaves as a normal secondary phase in rapidly solidified Cu-Cr_2Nb alloys, *i.e.*, conductivity has a maximum when plotted against temperature. This is further evidence that these alloys belong to the precipitation-hardened category.

The retention of mechanical strength up to high temperatures (*e.g.*, 1000 K) is a further advantage of DS copper as compared to precipitation-hardened or cold worked alloys. This high-temperature strength is ensured by good microstructural stability. The temperature variation of the tensile strengths of a number of dispersion-strengthened copper alloys produced by conventional and novel techniques is illustrated in Fig. 6.[15] This comparison reveals that mechanically distributed particles in thoria DS copper impart greater strength at high temperatures (1073 to 1270 K) than precipitates formed by solid state reactions (*e.g.*, *in situ* oxidation or precipitation from RS supersaturated solid solutions). Unfortunately, no such data on MA copper alloys with mechanically distributed particles are presently available. At moderately high temperatures (850 to 1150 K), the conventional alloys such as Narloy-Z and Cu-Cr and RS Cu-Cr-Nb alloys lose their strength because of particle growth, whereas thoriated copper and GLIDCOP alloys retain their strength, because the oxide dispersoids are thermodynamically stable. Moreover, the pinning effect of dislocations by stable oxide particles in GLIDCOP alloy Al-15 (0.7 vol% Al_2O_3) resulted in hardness retention following exposure up to 2000 hr at 1123 K (Fig. 7). MA Cu-15% Cr alloy also maintained its hardness of 240 HV after holding it 1 hr at temperatures up to 1273 K.[13] We note, however, that only a scatterband of hardness values vs temperature is given.

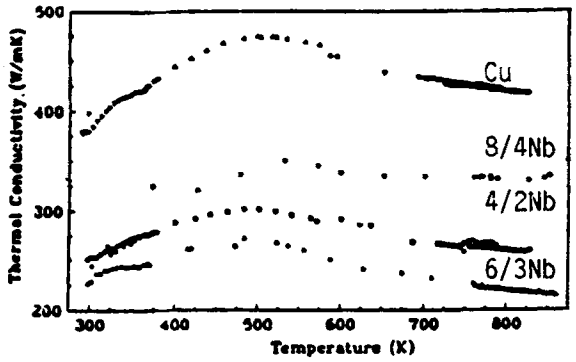

Fig. 5 Variation of thermal conductivity with temperature for various compositions of Cu-Cr_2Nb alloys. From Ref 15.

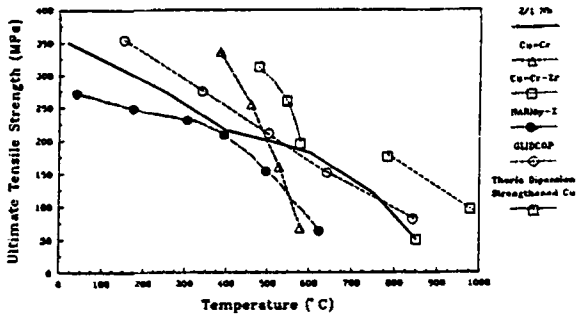

Fig. 6 Comparison of ultimate tensile strength of dispersion-strengthened copper alloys in the temperature range of 293 to 1273 K. 2/1 Nb is rapidly solidified Cu-Cr-Nb alloy; Cu-Cr, Cu-Cr-Zr and NARloy-Z are conventional wrought alloys; GLIDCOP is an internally oxidized alloy, and thoria dispersion-strengthened copper is obtained by a co-precipitation method. From Ref 15.

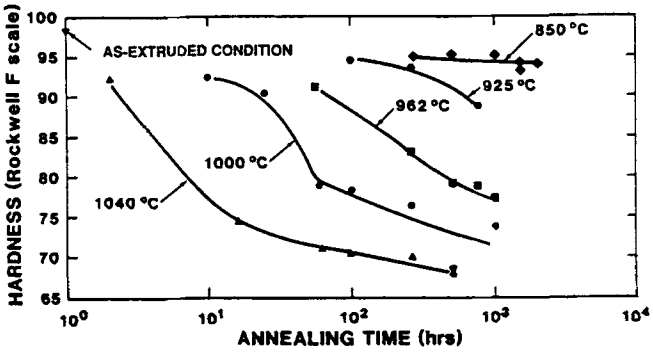

Fig. 7 Annealing response of low oxygen grade GLIDCOP Al-15. From Ref 31.

Therefore, because chromium particle growth is expected, it is difficult to discern the validity of this apparent stability.

For long-time applications of heat-resistant materials, the effect of dispersoids on creep strength is of prime importance. Although some studies of high-temperature properties of dispersion-strengthened copper single crystals have been published,[38] very few studies on creep properties of available DS copper alloys have been performed. The preliminary results

of Hayes *et al.*[11] show that the stress exponents and activation energies for creep of *in situ* processed Cu-Nb and Cu-Ta are similar to those reported for power law creep of pure Cu (n = 4-7). In contrast, creep tests on internally oxidized Cu-Al_2O_3 alloys showed higher stress exponents (n = 9-26) than pure copper, as expected in dispersion-strengthened metals.[3,32] To rationalize the high stress exponents in dispersion-strengthened materials, the creep rate may be described by a modified Dorn equation:[39]

$$\dot{\varepsilon} = A\left(\frac{\sigma - \sigma_o}{E}\right)^n \exp\left(\frac{-Q_c}{k_B T}\right) \quad [3]$$

in which $\dot{\varepsilon}$ is the strain rate, A is a material dependent constant, σ is the applied stress, σ_o is the threshold stress, E is the plastic modulus, n is the stress exponent, T is the absolute temperature, Q_c is the appropriate activation energy for deformation in the temperature range of interest and k_B is the Boltzmann constant. By introducing the threshold stress, the value of n can be reduced so that the theoretical description of dislocation motion past incoherent dispersoids may be applied. This threshold stress may be important on its own as a design-limiting strength property.[1] If service stresses are below the threshold stress, creep deformation is minimized. The threshold stress has found a physical interpretation and is generally some fraction of the Orowan stress:

$$\sigma_{0r} = 0.84\frac{MGb}{2\pi(1-\nu)^{0.5}\lambda}\ln\left(\frac{r}{b}\right) \quad [4]$$

where M is the Taylor factor, G is the shear modulus, b is the Burgers vector, ν is the Poisson ratio, λ is the mean particle spacing, and r is the mean particle radius.

Although the origin of a threshold stress was first attributed to localized dislocation climb over the particle, Artz and co-workers have recently developed a new theoretical description of creep of dispersion-strengthened alloys that better fits the creep experimental data.[1,40,41] This model describes creep of dispersion-strengthened alloys by considering that dislocations are pinned on the departure side of particles. An attractive interaction between the dislocation and particle/matrix interface was experimentally observed and leads to a detachment stress given by:

$$\sigma_D = \sqrt{1-k^2}\,\sigma_{0R} \quad [5]$$

where k is an interaction parameter. No relaxation takes place, nor is there a particle/dislocation interaction for $k = 1$. This is the case when the matrix and particle fit perfectly, or when particles are coherent. At the other end of the spectrum, a strong attractive interaction occurs when $k = 0$, and the dislocation completely relaxes its energy. The detachment process is thermally activated, and the time for this detachment is significant in comparison to the time required for a dislocation to move from one particle to another and to climb over the new particle. Based on this assumption, Artz and co-workers developed a new equation for creep rate:

$$\dot{\varepsilon} = \dot{\varepsilon}_o \exp\left[-\frac{Gb^2 r}{k_B T}(1-k)^{3/2}\ (1-\frac{\sigma}{\sigma_D})^{3/2}\right] \quad [6]$$

in which $\dot{\varepsilon}_o$ is a reference strain rate equal to $3D_v \rho \lambda/b$, where D_v is the volume diffusivity, and ρ is the density of mobile dislocations.

The new equation for creep has valuable predictive capabilities for the design of high-temperature strength materials. First, the threshold-like behavior is predicted, although creep Eq 6 contains no explicit threshold value (Fig. 8). As already noted, the threshold stress implies that materials can be used under some finite load at extreme temperatures without deformation. Second, the interaction parameter should be as low as possible. Its value depends on the particle/matrix interfacial properties and material. For instance, Rosler and Artz found that Al_4C_3 obtained by mechanical alloying has a stronger interaction (k = 0.75) with the aluminum matrix than Al_xFe_yCe (k = 0.95) obtained by rapid solidification.[40] They argue that carbides are poorly bonded with the aluminum matrix, thereby strongly attracting dislocations at high temperatures. They conclude paradoxically that weakening of the interfacial bonding results in highly attractive, therefore efficient, dispersoids. Furthermore, they suggest possibilities to influence interfacial bonding by segregation alloying, dispersoid pretreatment, or the processing route itself. In the latter case, preliminary experiments indicated that MA iron-base alloys are more creep resistant than internally oxidized alloys with similar composition and microstructure.[41] The explanation stems from strong interfacial bonding of dispersoids in internal oxidation as required by the nucleation process. Further studies on the relationship between interfacial bonding and k parameter values will strongly enhance the chances of selecting the best dispersoids and processing routes to ensure high-temperature strength. Such k values in differently processed copper alloys are currently sought. Third, the detachment model predicts an optimum particle size at a given temperature, volume fraction, and strain rate, whereas the climb model requires continuous smaller spacing. The optimum particle size is given by:

$$\left(\frac{r}{b}\right)_{\text{opt}} = \left[\frac{5}{3(1-k)}\right]^{3/2}\frac{[\ln(\dot{\varepsilon}_o/\dot{\varepsilon})\,k_B T]}{Gb^3} \quad [7]$$

A plot of creep strength vs particle radius according to Rosler-Artz theory for pure copper dispersion strengthened with various particle volume fractions assuming a value of k = 0.9 is given in Fig. 8. As expected, attaining optimum particle size may be more efficient than increasing the volume fraction. For example, the same strength may be achieved by decreasing particle size from 40b to (10 to 20)b or doubling volume fraction from 5 to 10%. As already shown, a low volume fraction is beneficial for high-conductivity alloys.

6 Summary

This review covers state-of-the-art heat-resistant, high conductivity dispersion-strengthened copper alloys based on the understanding of the basic microstructure/properties relationship. Although many of these materials have high strength levels

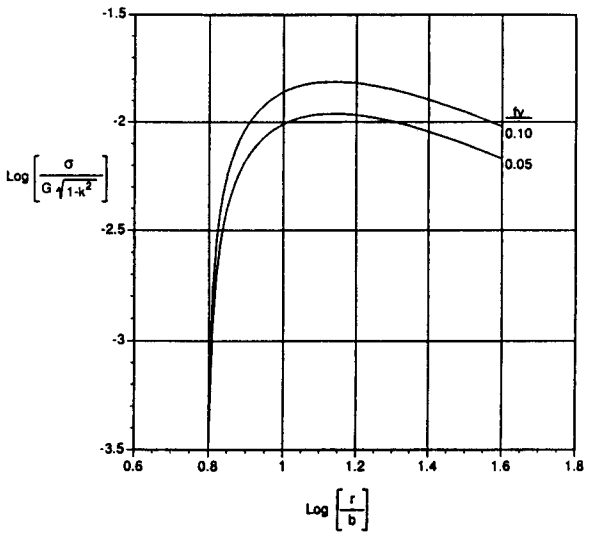

Fig. 8 Optimum particle size as seen in a plot of creep strength (for achieving $\dot{\varepsilon} = 10^{-8}\ s^{-1}$) vs particle radius for different volume fractions of a dispersoid that has $k = 0.90$ in copper matrix ($G = 34.2$ GPa, $b = 2.56 \times 10^{-10}$m); $T = 773$ K, $\rho = 10^{13}\ m^{-2}$.

associated with good thermal conductivities, still better materials are needed. The author believes that any improvement in physical and mechanical properties is worthwhile pursuing and will lead to innovation in the design and use of copper alloys. The current theoretical understanding of high-temperature strength and conductivity outlined above has important implications for future alloy design. Bearing this in mind, the best combination of high-temperature strength and high conductivity may be obtained by:

- Selection of dispersoids based on their high-temperature stability, resistance to coarsening, maximum interaction with the matrix, and physical and mechanical properties
- Designing the optimum volume fraction f as a trade-off between high thermal conductivity and high-temperature strength
- Designing the optimum particle size and grain size to maximize high-temperature strength for a specific application
- Using the appropriate processing method leading to even distribution of optimum size particles in a matrix with a certain grain size and to microstructural stability

The latter requires a better understanding of nonequilibrium processing technology such as mechanical alloying. Finally, a more detailed characterization of properties of existing and potential dispersion-strengthened copper alloys will make their design and application more complete.

Acknowledgment

The author is indebted to Professor J.C. Gibeling for valuable discussion and critical reading of the manuscript.

References

1. J. Rosler and E. Artz, *Acta Metall., 38*, 671-683 (1990).
2. N. Fuschillo and M.L. Gimpl, *J. Appl. Phys., 43*, 5513-5516 (1971).
3. A.V. Nadkarni, in *High Conductivity Copper and Aluminum Alloys*, E. Ling and P.W. Tautenblat, Ed., TMS-AIME, Warrendale, PA, 77 (1984).
4. J.G. Schroth and V. Franetovic, *Journal of Materials, 41*(1), 37-39 (1989).
5. M.A. Morris and D.G. Morris, *Mater. Sci. Eng., A111*, 115-127 (1989).
6. G.B. Schaffer and P.G. McCormick, *Scripta Metall., 23*, 835-838 (1989).
7. T. Takahashi, Y. Hashimoto, K. Koyama, and K. Suzuki, in *Proc. 4th Intern. Symp. Science and Technology of Sintering*, S. Somiya *et al.*, Ed., Elsevier Applied Science, London, 659 (1987).
8. T. Takahashi and Y. Hashimoto, *J. Jpn. Inst. Met., 54*, 67-75 (1990).
9. J.J. Stephens and C.R. Hills, "Long Term Stability of Two Dispersion Strengthened Copper Alloys at Elevated Temperatures," presented at the 119th Annual Meeting of TMS, Anaheim, Feb 18-22 (1990).
10. N.W. Blossom, *Met. Powder Rep.*, Jul/Aug, 55 (1990).
11. R.W. Hayes, L.G. Fritzemeier, and P.D. Krotz, "Steady-State Creep Behavior and Microstructure Stability of a Cu Based High Strength-High Thermal Conductivity Microcomposite," presented at Aeromat, '90, Long Beach (1990).
12. M.A. Morris and D.G. Morris, *Mater. Sci. Eng., A104*, 201-213 (1990).
13. A.N. Patel and S. Diamond, *Mater. Sci. Eng., 98*, 329-334 (1988).
14. M.A. Morris and D.G. Morris, *Scripta Metall., 24*, 1701-1706 (1990).
15. D.L. Ellis and G.M. Michal, "Precipitation Strengthened High Strength, High Conductivity Cu-Cr-Nb Alloys Produced by Chill Block Melt Spinning," NASA Technical Memorandum 185144 (1989).
16. D.L. Ellis, G.M. Michal, and N.W. Orth, *Scripta Metall., 24*, 885-890 (1990).
17. A.V. Nadkarni and J.E. Synk, in *Metals Handbook, Powder Metallurgy*, vol 7, 9th ed., ASM, 711 (1984).
18. J.S. Benjamin, in *New Materials by Mechanical Alloying Techniques*, E. Artz and L. Schultz, Ed., DGM Informationsgesellschaft, Oberursel, 3 (1989).
19. G.B. Schaffer and P.G. McCormick, *Met. Trans., 21A*, 2789-2794 (1990).
20. T. Takahashi, Y. Hashimoto, S. Omori, and K. Koyama, *Trans. J. Inst. Met., 26*, 271-279 (1985).
21. E.P. Daneliya, M.D. Teplitskii, and V.I. Solopov, *Fiz. Met. Metallov., 47*, 595-597 (1979).
22. M.L. Adams, S.L. Kampe, A.R. Harmon, and L. Christodoulou, in *1989 Advances in Powder Metallurgy*, T.G. Gasbarre and W.F. Jandeska, Jr., Ed., vol 3, 439, MPIF, APMI, Princeton, NJ (1989).
23. H. Gray, personal communication, NASA Lewis Center, Cleveland, OH (1990).
24. F.H. Froes, *Met. Powder Rep.*, 838-840 (1988).
25. R.N. Wright and I.E. Anderson, *Mater. Sci. Eng., A114*, 167-172 (1989).
26. R.W. Balliett, personal communication, NRC, Inc., Newton, MA (1990).
27. D.G. Morris and M.A. Morris, in *New Materials by Mechanical Alloying Techniques*, E. Artz and L. Schultz, Ed., DGM Informationsgesellschaft, Oberursel, 143 (1989).
28. I.M. Lifshitz and V.V. Slyozov, *J. Phy. Chem. Solids, 19*, 35-50 (1961).

29. C. Wagner, *Z. Electrochem.*, *65*, 581-591 (1961).
30. G.L. Shiflet and J.A. Hawk, in *Dispersion Strengthened Aluminum Alloys*, Y.-W. Kim and W.M. Griffin, Ed., TMS, Warrendale, PA, 31 (1988).
31. J.J. Stephens, J.A. Romero, and C.R. Hills, in *Microstructural Science*, H.J. Cialoni *et al.*, Ed., vol 16, 245-264 (1988).
32. J.J. Stephens, R.J. Bourcier, F.J. Vigil, and D.T. Schmale, in "Mechanical Properties of Dispersion Strengthened Copper: A Comparison of Braze Cycle Annealed and Coarse Grain Microstructures," SANDIA Report, SAND 88-1351 (1988).
33. M. Slesar, G. Jangg, M. Besterci, J. Durisin, and M. Orolinova, *Z. Metallkunde.*, *80*, 817-824 (1989).
34. K. Schroeder, in *High Conductivity Copper and Aluminum Alloys*, E. Ling and P.W. Tautenblat, Ed., TMS-AIME, Warrendale, PA, 1 (1984).
35. J.S. Benjamin and M.J. Bomford, *Met. Trans*, *8A*, 1301-1305 (1977).
36. S. Gidea and J. Groza, *Metall. Proc. Bucharest Polytechnic Inst.*, *1*, 17-27 (1973).
37. K.R. Karasek and J. Bevk, *Scripta Metall.*, *13*, 259-262 (1979).
38. R.S.W. Shewfelt and L.M. Brown, *Philos. Mat.*, *35*, 945-962 (1977), *30*, 1135-1145 (1974).
39. J.C. Gibeling and W.D. Nix, *Mater. Sci. Eng.*, *45*, 123-135 (1980).
40. J. Rosler and E. Artz, in *New Materials by Mechanical Alloying Techniques*, E. Artz and L. Shultz, Ed., DGM Informationsgesellschaft, Oberursel, 279 (1989).
41. E. Artz, in *New Materials by Mechanical Alloying Techniques*, E. Artz and L. Schultz, Ed., DGM Informationsgesellschaft, Oberursel, 185 (1989).